


pH-sensitive polymeric nanoparticles of mPEG-PLGA-PGLu with hybrid core for simultaneous encapsulation of curcumin and doxorubicin to kill the heterogeneous tumour cells in breast cancer

Jian-Dong Yuan, De-Li ZhuGe, Meng-Qi Tong, Meng-Ting Lin, Xia-Fang Xu, Xing Tang, Ying-Zheng Zhao & He-Lin Xu


To cite this article: Jian-Dong Yuan, De-Li ZhuGe, Meng-Qi Tong, Meng-Ting Lin, Xia-Fang Xu, Xing Tang, Ying-Zheng Zhao & He-Lin Xu (2018) pH-sensitive polymeric nanoparticles of mPEG-PLGA-PGLu with hybrid core for simultaneous encapsulation of curcumin and doxorubicin to kill the heterogeneous tumour cells in breast cancer, *Artificial Cells, Nanomedicine, and Biotechnology*, 46:sup1, 302-313, DOI: [10.1080/21691401.2017.1423495](https://doi.org/10.1080/21691401.2017.1423495)



To link to this article: <https://doi.org/10.1080/21691401.2017.1423495>

 View supplementary material 



 Published online: 04 Jan 2018.

 Submit your article to this journal 

 Article views: 2293

 View related articles 

 View Crossmark data 

 Citing articles: 27 View citing articles 



pH-sensitive polymeric nanoparticles of mPEG-PLGA-PGlu with hybrid core for simultaneous encapsulation of curcumin and doxorubicin to kill the heterogeneous tumour cells in breast cancer

Jian-Dong Yuan^{a*}, De-Li Zhu^{b*}, Meng-Qi Tong^b, Meng-Ting Lin^b, Xia-Fang Xu^b, Xing Tang^c, Ying-Zheng Zhao^b and He-Lin Xu^{a,b}

^aDepartment of Orthopaedics, the First Affiliated Hospital of Wenzhou Medical University, Wenzhou, Zhejiang, People's Republic of China;

^bDepartment of Pharmaceutics, School of Pharmaceutical Sciences, Wenzhou Medical University, Wenzhou City, Zhejiang Province, China;

^cDepartment of Pharmaceutics, College of Pharmacy, Shenyang Pharmaceutical University, Shenyang, Liaoning, PR China

ABSTRACT

Most breast tumours are heterogeneous and not only contain the bulk of differentiated tumour cells but also a small population of highly tumorigenic and intrinsically drug-resistant cancer stem cells (CSCs). Herein, a pH-sensitive nanoparticle with simultaneous encapsulation of curcumin and doxorubicin (CURDOX-NPs) was prepared by using monomethoxy (polyethylene glycol)-b-P (D,L-lactic-co-glycolic acid)-b-P (L-glutamic acid) polymer to simultaneously target the differentiated tumor cells and CSCs. CURDOX-NPs had a mean diameter of 107.5 nm and zeta potential of -13.7 mV, determined by DLS. Drug-loading efficiency for curcumin and doxorubicin was reaching to 80.30% and 96.2%, respectively. Moreover, a cascade sustained-release profiles with the faster release of CUR followed by a slower release of DOX was observed in normal pH7.4 condition. Moreover, a pH-sensitive release profile for each cargo was seen in pH5.0 condition. The anti-tumour effect of CURDOX-NPs on CSCs-enriching MCF-7/ADR mammospheres was confirmed by *in vitro*. Moreover, a significant regression of tumour growth after treatment with CURDOX-NPs was also observed in Xenograft mice model. The percentage of CSCs in tumour significantly decreased from 39.9% in control group to 6.82% after treatment with CURDOX-NPs. The combinational delivery of CUR and DOX may a potentially useful therapeutic strategy for refractory breast cancer.

ARTICLE HISTORY

Received 21 November 2017

Revised 26 December 2017

Accepted 28 December 2017

KEYWORDS

Curcumin; doxorubicin; block copolymer; nanoparticles; poly(L-glutamic acid); poly(D,L-lactic-co-glycolic acid); multi-drugs resistance

Introduction

Breast cancer is the most common cancer diagnosed in women and is the second most frequent cause of cancer mortality in western women [1]. Current breast tumour therapies including surgical resection, chemotherapy or radiotherapy mainly focus on bulk population reduction of tumour cells, any of which was not able to prevent the relapse and metastasis of breast cancer [2]. Recently, most breast tumours are heterogeneous and contain small population of highly tumorigenic and intrinsically drug resistant cancer stem cells (CSCs). CSCs are thought to constitute a small subset of cells within a tumour that both initiate relapse and metastasis of cancer because of their capacity for self-renewal and inherent chemo- and radio-resistance and give rise to an increase in non-tumorigenic cancer cell progeny population through differentiation. In breast cancer, these cells, variously termed breast cancer stem cells (CSCs) or tumour-initiating cells (TICs), are distinguished by characteristic markers, such as the cell surface antigens $CD44^{high}/CD24^{low}$ or ALDH1 enzymatic activity. CSCs often overexpress drug efflux transporters,

spend most of their time in non-dividing G_0 cell cycle state, and therefore, can escape the conventional chemotherapies [2]. Thus, targeting CSCs is essential for developing novel therapies to prevent cancer relapse and emerging of drug resistance.

Doxorubicin (DOX), an anthracycline cationic antibiotic, has been used as first-line drug against a wide range of human cancers including breast cancer, lymphadenoma and many types of soft tissue sarcomas [3,4]. However, multiple exposure of DOX usually resulted in tumour drug resistance and severe cardiac toxicity, which limited its broad application in clinics. A variety of nanocarriers have been developed to overcome these limitations. Liposome (Doxil®), polymeric micelles (SP1049C® and NK911®) has been approved by FDA to overcome these drawbacks of DOX [5]. For example, Doxil® successfully can significantly prolong *in vivo* retention time of DOX, reduce its cardiac toxicity and raise the maximum tolerate dose during therapeutic process. However, the anti-tumour effect of Doxil® against most of tumours including breast cancer, especially for refractory drug-resistant breast tumours, was not significantly enhanced accordingly.

CONTACT H-L. Xu ✉ xhlpharm1214@126.com ☎ School of Pharmaceutical Sciences, Wenzhou Medical University, Wenzhou City, Zhejiang Province 325035, China

*These authors contributed equally to this work.

Supplemental data for this article can be accessed [here](#).

© 2018 Informa UK Limited, trading as Taylor & Francis Group

Inversely, the dangerous side effect called the hand foot syndrome was produced because the long circulation time of Doxil[®] *in vivo* increased the distribution of DOX to normal skin tissue [6]. Alternatively, SP1049C[®] prepared by Pluronic L61 and L127 at 1:8 molar ratios is a micelle preparation with physical encapsulation of DOX [7]. SP1049C[®] has been evaluated in stage of clinical phase II for refractory drug-resistant breast cancer in view of the ability of Pluronic to overcome the multi-drug resistance. However, because DOX was physically encapsulated in pluronic-based micelles through the weak hydrophobic interaction, its *in vivo* pharmacokinetics was not significantly improved as indicated in stage of clinical phase-I study. The blood AUC value of SP1049C[®] was only 12.5% higher than that of the common DOX solution product, and severe cardiac toxicity was still existing [8].

Curcumin (CUR), a kind of lipophilic active ingredient, is a low-molecular-weight polyphenol compound derived from the rhizome of the plant *Curcuma longa* [9]. Recently, several researchers have found that CUR and its derivants have the anti-tumour activity to increase the sensibility of multiple first-line chemotherapeutic drugs to drugs-resistant tumour [10]. Besides, several reports have showed that CUR could act on ROS-MAPK and NF- κ B-signalling pathway, thus inhibiting growth of three-negative breast cancer, breast cancer stem cells and hindering permanent inactivation of drug-resistant pump, P-gp [11]. CUR has been approved for the clinical prevention of tumour drug resistance. It has been reported that the use of CUR as a chemical sensitizer in combination with doxorubicin or other first-line chemotherapeutics can improve its anti-tumour efficacy and reduce its cardiac toxicity [12]. Especially, there is a growing concern for the ability of CUR to induce apoptosis of cancer stem cells in many cancer types including breast cancer [13], liver cancer [14]. It was reported that CUR treatment also specifically targeted CSC-like cell population via inhibiting Wnt/ β -catenin and Sonic Hedgehog pathways, the suppression of CD44⁺/CD24⁻ and CD49f⁺/CD24⁺ subpopulations and the subsequent impairment of mammosphere formation [15]. But the clinical application of CUR via oral administration was limited by its low bioavailability [16]. Besides, it was also difficult to be administrated by intravenous injection due to its low water solubility [17].

In our previous study, a novel triblock copolymer, monomethoxy (polyethylene glycol)-b-P (D,L-lactic-co-glycolic acid)-b-P (L-glutamic acid) (mPEG-PLGA-PGlu), was successfully synthesized. It was discovered that mPEG-PLGA-PGlu copolymer was self-assembled into nanoparticles with a hybrid core of PLGA and PGlu, and a PEG shell through controlling the length of each block. Moreover, the self-assembled nanoparticles of mPEG_{5k}-PLGA_{20k}-PGlu (60) polymer (subscript number denotes the molecular weight of each block; *k* denotes 1000 Da; number in brackets denoted the number of the repeating number of L-glutamic units) were specifically responsive to an endosomal pH of 5.0–6.0 due to the configuration transition of the PGlu segment [18]. The model drug, DOX, could be easily loaded into the hybrid-core nanoparticles with a high drug loading of 25% through electrostatic interaction with PGlu segment [19]. Considering the existence of hydrophobic PLGA block, the hydrophobic model

drug, CUR, is also expected to be encapsulated inside hybrid core of mPEG-PLGA-PGlu nanoparticles through hydrophobic interaction.

In this study, a pH-sensitive dual drug-loaded nanoparticle (CURDOX-NPs) was prepared by using mPEG-PLGA-PGlu polymer to simultaneously target the breast cancer stem cells and the differentiated tumour cells. The particle size, surface potential, morphology and drug-loading capability of CURDOX-NPs were carefully characterized *in vitro*. The effective anti-tumour effect of CURDOX-NPs was also confirmed by *in vitro* and *in vivo*. Additionally, the ability of CURDOX-NPs to kill the heterogeneous tumour cells in tumour tissues was also evaluated *in vitro* tumour spheroid and *in vivo* Xenograft mice model.

Material and methods

Materials

mPEG_{5k}-PLGA_{20k}-PGlu (60) was synthesized according to our previous publications. Curcumin (CUR, purity of 98%) were purchased from WAKO (Japan); Doxorubicin (DOX, purity of 98%) was purchased from Beijing HVSF united chemical materials company (Beijing, China). RPMI-1640 culture medium, foetal bovine serum (FBS), diastase and digestive enzyme (TRYPsin) were purchased from GIBCO Corporation (USA); methyl thiazolyl tetrazolium (MTT) and DAPI were purchased from sigma (USA).

Preparation of dual drug-loaded polymer nanoparticles

The drug-loaded nanoparticles were prepared by nanoprecipitation method. In brief, curcumin and mPEG-PLGA-PGlu copolymer were firstly co-dissolved in 6 ml *N,N*-dimethyl formamide (DMF) under magnetic stirring as organic phase. Afterward, 4 ml aqueous solution of doxorubicin hydrochloride was slowly dripped into the organic phase under vigorous stirring, and the mixed system continued reacting for 30 min. And then, the reaction mixture was dialyzed (M_w cut-off, 3500 Pa) against distilled water for 24 h to remove the organic phase, and distilled water was replaced four times (3, 6, 12 and 24 h) during dialysis. Finally, the mixture was centrifuged to remove the drug precipitation at a speed of 12,000 rpm and the supernatant drug-loaded nanoparticles were collected for study. Series of formulations were prepared by changing the amount of total drugs or copolymer in formulations. In each formulation, the molar ratio of CUR/DOX was controlled at 1:1, and total drugs/copolymer was fixed to be 1:20. As controls, the single drug-loaded nanoparticles including CUR-loaded nanoparticles or DOX-loaded nanoparticles were also prepared by the similar procedure above.

The drug-loading content and encapsulation efficiency

The loading content (DL) and entrapment efficiency (EE) of drug-loaded nanoparticles were determined by HPLC assay after destroying the nanoparticles. Briefly, 100 μ L drug-loaded nanoparticles was added to 3 ml acetonitrile in a volumetric

flask, and further sonicated to destroy the nanoparticle. After filtration through a membrane with pore size of 0.8 μm , the filtrate was detected by HPLC (Hitachi L-2130 pump, L-2400 UV-Vis spectrophotometer). HPLC condition was listed as follow: Eclipse XDB-C18 column (250 mm \times 4.6 mm, 5 μm); mobile phase: acetonitrile-water (60:40, v/v); flow speed of 1.0 ml/min; detect waver at 210 nm; column temperature of 25 $^{\circ}\text{C}$. The drug-loading content, DLC(%) and the drug-loading efficiency, DLE(%) were calculated by the following equations, respectively. $\text{DLC}\% = \text{weight of the drug in nanoparticles} / (\text{weight of the feeding polymer} + \text{weight of drug}) \times 100\%$; $\text{DLE}\% = (\text{weight of the practical drug in nanoparticles} / \text{weight of the feeding drug}) \times 100\%$.

Particle size and morphology of drug-loaded nanoparticles

The size and Zeta potential of the prepared nanoparticles were determined by dynamic light scattering (DLS). The nanoparticles solutions were first filtered through a 0.8 μm disposable membrane filter prior to measurement and were determined p by NICOMPTM 380 with the laser wavelength at 632.8 nm and a scatter angle of 90 $^{\circ}$ at room temperature after proper dilution. The morphology of the nanoparticles was examined using a JEOLJEM-2000EX transmission electron microscope (100 kV accelerating voltage) with phosphotungstate acid solution (2%, w/w) staining.

DSC and fluorescent spectrum

In order to analyse the status of the encapsulated drugs in polymeric nanoparticles, the lyophilized powders of nanoparticles solution were determined by calorimeter (Mettler Toledo, Switzerland) equipped with a refrigerated cooling system. Samples (approximately 5 mg, accurately weighed) including DOX-HCl, CUR, mPEG-PLGA-PGlu copolymer, physical mixtures of (DOX + CUR + mPEG-PLGA-PGlu copolymer) and lyophilized CURDOX-NPs, were analysed at heating temperature ranging from -30°C to 300°C with a linear heating rate of 5 $^{\circ}\text{C}/\text{min}$.

To investigate the localization of DOX in the nanoparticles, the fluorescence spectra of the drug-loaded nanoparticles were recorded before and after incubation with equivalence of DMF. The excitation wavelength was fixed at 480 nm, and the emission spectrum of DOX was recorded from 500 to 720 nm at a scan speed of 2 nm/s.

In vitro release profiles of DOX and CUR from CURDOX-NPs

The release profiles of CUR and DOX from nanoparticles were performed at 37 $^{\circ}\text{C}$ using a dialysis method depicted in literature [20]. Briefly, 2 ml of CURDOX-NPs solutions were placed in a dialysis bag (cut off, 3500), hermetically sealed and the bulk dialysis bag was immersed into 50 ml of release medium (pH7.4 PBS or pH5.0 acetate buffer) containing 1% (v/v) SDS under continuous shaking at 100 rpm. At predetermined time intervals, 1 ml of release medium was withdrawn for analysis.

Meanwhile, an equal volume of fresh PBS was supplemented to maintain the constant release medium. The concentration of CUR and DOX were analysed by HPLC method described earlier. The cumulative release percentage (%) was determined by dividing the cumulative amount of DOX/CUR recovered in the dialysis medium by the total amount in the nanoparticles.

In vitro cytotoxicity of CURDOX-NPs against MCF-7/ADR cells

In vitro culture of MCF-7/ADR cells

Human breast carcinoma cells (MCF-7) and doxorubicin-resistant human breast carcinoma cells (MCF-7ADR) were purchased from Nanjing Kaiji Biotech. Ltd. Co. (Nanjing, China). MCF-7 cells were cultured in RPMI-1640 supplemented with 10% FBS, while DOX (1 $\mu\text{g}/\text{mL}$) was supplemented in RPMI-1640 containing 10% of FBS for culture of MCF-7/ADR. Cells were cultured in a humidified atmosphere at 37 $^{\circ}\text{C}$ with 5% CO_2 . The cells were subcultured with 0.25% trypsin-EDTA after reaching 85% of confluence.

Cytotoxicity assay

In order to demonstrate the reversal of multidrug resistance by curcumin, *in vitro* cellular toxicity of free DOX solution (DOX-S), DOX-NPs, CUR-NPs and CURDOX-NPs against the sensitive MCF-7 cells and resistant MCF-7/ADR cells was assayed by the MTT method. MCF-7 cells or MCF-7/ADR cells were seeded at 8×10^3 cells/well in 96-well plates and allowed to grow overnight in culture medium. Afterward, 100 μL of RPMI-1640 medium containing free drugs or equivalent drugs-loaded nanoparticles were added to the plate for 48 h. Then, the culture medium was removed, replaced with 90 μL fresh medium and 10 μL MTT solution (5 mg/mL) and further incubated for 4 h under normal growth conditions. After incubation, MTT was removed and 200 μL DMSO was added to dissolve the formazan. The absorbance was assayed at 492 nm in a microplate reader. As a control, cells were grown in culture medium in the absence of drugs, and three wells were set in each group. The cell survival rate was calculated according to the following formula: cell survival rate (%) = $(A_{\text{test}}/A_{\text{control}}) \times 100\%$; A_{test} : Absorbance of test group; A_{control} : Absorbance of control group. Meanwhile, IC_{50} value, the drug concentration at cell viability of 50% was calculated by modified Curtis's method.

Cellular uptake studies

MCF-7/ADR cells were seeded at a density of 1×10^3 in 6-well culture plates and grow overnight. The medium was replaced with a fresh medium including free DOX solution (DOX-S) or DOX-NPs/CURDOX-NPs with an equivalent DOX concentration (10 $\mu\text{g}/\text{mL}$) for a further 4-h incubation. Then, the cells were washed three times with ice-cold PBS and fixed with 4% paraformaldehyde for 20 min. The nuclei were then counterstained with DAPI for 5 min. The cells were rinsed three times with PBS, and closed by 70 μL 50% glycerol for laser confocal microscopy. As a control, the *in vitro* cellular uptake

of DOX-S, DOX-NPs and CURDOX-NPs by the sensitive MCF-7 cells was also evaluated.

Toxicity of CURDOX-NPs against tumour spheroid of MCF-7/ADR

Culture of MCF-7/ADR tumour spheroid and identification of breast cancer stem cells

MCF-7/ADR mammospheres were developed using the liquid overlay method as previously described. In brief, MCF-7/ADR cells were seeded into 48-well plates pre-coated with 2% agarose hydrogel at a density of 4×10^3 cells per well and cultured for several days at 37 °C in the presence of 5% CO₂. The compact MCF-7/ADR spheroids were selected for subsequent experiments after 7 days of culture.

MCF-7/ADR mammospheres were collected for identifying phenotype and purity of MCF-7 cancer stem cells. Briefly, the mammospheres were enzymatically dissociated by adding trypsin (0.25%, g/100 ml), washed with cold PBS (pH 7.4) and simultaneously stained with 5 ml anti-CD44-FITC and 5 ml anti-CD24-PE at 4 °C for 30 min in the staining buffer (PBS pH 7.4). The sample was then washed three times with cold PBS (pH 7.4) and resuspended in 500 ml of cold PBS and assayed on a FACScan flow cytometer (Becton Dickinson, San Jose, CA). Side scatter and forward scatter profiles were used to eliminate cell doublets.

Growth inhibition of MCF-7/ADR mammospheres and killing the heterogeneous cells in mammospheres

MCF-7/ADR mammospheres were treated with CUR-NPs (equivalent CUR concentration of 40 µg/mL) or DOX-NPs (equivalent DOX concentration of 40 µg/mL) or CURDOX-NPs (equivalent CUR and DOX concentration was 18.2 µg/mL and 21.8 µg/mL, respectively). Flesh DMEM medium was served as negative control. At different time point after treatment, MCF-7/ADR mammospheres were observed with an inverted microscope (Chongqing Optical & Electrical Instrument Co. Ltd., Chongqing, China). The length diameter (d_{\max}) and width diameter (d_{\min}) of each spheroid were measured every day for 3 days. The spheroid volume (V) was calculated using the following formula: $V = 0.5 \times d_{\max} \times d_{\min}^2$.

In vivo anti-tumour effect

The dissociated MCF-7/ADR mammosphere cells at a density of 3×10^6 cells were injected subcutaneously into the right flank region of Balb/c nude mice. When the tumour volume grew to approximately 100 mm³, the mice were randomly assigned to a control (saline) group, CUR-NPs group, DOX-NPs group and CURDOX-NPs, each group containing six mice. Different formulations were given at the same drug dose of 2.5 mg/kg and administered intravenously through the tail vein every other day four times in all. The body weight and tumour size were measured and recorded every other day after administration. Tumour volume was calculated by the following formula: $V = (L \times W^2)/2$. W and L were the minor and maximum axes of the tumour, respectively. Mice were

sacrificed on the 18th day, and the tumour weight was measured to evaluate the antitumor effect.

Analysis of cancer stem cells in tumours after treatments

At the end of the treatment, tumours were collected from all groups and washed 3 times by PBS. After the tumours were cut into 1 mm³ of small pieces, enzymatic digestion was performed by using collagenase III at 37 °C for 2 h. To obtain single cells, cell suspension was filtered through a 40-µm cell strainer. Cells were washed three times with PBS, re-suspended in 100 ml of cold PBS, and stained with anti-human CD44-FITC and CD24-PE on ice for 30 min. After washed three times with cold PBS, the cells were suspended in 400 ml of cold PBS and the percentage of cancer stem cells (CD44⁺/CD24⁻) was analyzed by flow cytometry using the FACScan instrument.

Toxicity of CURDOX-NPs against normal tissues

To evaluate the toxicity of CURDOX-NPs, the rats were sacrificed at the end of treatment, and samples of heart, liver, spleen, lung and kidney were collected and routinely stained with haematoxylin and eosin (HE).

Statistical analysis

Student's t -test was used to evaluate the statistical significance of differences between formulations. Value was denoted as mean \pm standard deviation (SD) and the data were considered statistically significant at $p < .05$.

Results and discussions

Preparation and characterisation of dual drug-loaded mPEG-PLGA-PGlu nanoparticles

In our previous, amphiphilic mPEG-PLGA-PGlu copolymer was easily self-assembled into negatively charged nanoparticles with a hybrid core of PLGA and PGlu, and a stealth PEG shell by the classical nanoprecipitation method. Moreover, a high drug loading of ca.25% for doxorubicin hydrochloride was reached through electrostatic interaction with the negative hybrid-core. In this study, the poorly soluble CUR was firstly dissolved in DMF together with mPEG-PLGA-PGlu copolymer as organic phase, rendering occurrence of hydrophobic interaction between CUR and PLGA segment. When aqueous DOX solution was added to organic phase, two phenomena, that was, CUR-binding PLGA segments was separated from organic phase and hydrophobic electrostatic complex between DOX and PGlu segment was instantaneously formed, dominated co-encapsulation of CUR and DOX in hybrid core of nanoparticles. In order to explore drug-loading content and encapsulating efficiency of mPEG-PLGA-PGlu nanoparticle, series of formulations were prepared by changing the amount of total drugs or copolymer in formulations. The results were shown in Table 1. A high encapsulating

Table 1. Characteristics of various formulations of nanoparticles ($n = 3$, mean \pm SD).

| No | Polymer(mg) | Total drug (mg) (DOX + CUR) | DLC (%) | | DLE (%) | | D_h (nm) | Zeta potential |
|-------------|-------------|--------------------------------|-----------------|-----------------|------------------|------------------|-----------------|-----------------|
| | | | CUR | DOX | CUR | DOX | | |
| Blank NPs | 200 | – | – | – | – | – | 211.2 ± 1.3 | -25.4 ± 0.2 |
| DOX-NP | 200 | 2.5 ± 2.5 | – | 2.28 ± 0.34 | – | 95.00 ± 1.89 | 102.1 ± 0.4 | -21.2 ± 0.6 |
| CUR-NP | 200 | 2.5 ± 2.5 | 1.87 ± 0.41 | – | 76.91 ± 2.56 | – | 228.5 ± 1.5 | -23.8 ± 0.3 |
| DOXCUR-NP-1 | 100 | 5 ± 5 | 2.61 ± 0.12 | 4.31 ± 0.14 | 57.73 ± 2.32 | 95.66 ± 3.35 | 56.2 ± 0.2 | -5.2 ± 0.2 |
| DOXCUR-NP-2 | 200 | 5 ± 5 | 1.81 ± 0.04 | 2.28 ± 0.11 | 72.94 ± 3.45 | 95.80 ± 2.15 | 102.1 ± 0.1 | -11.2 ± 0.1 |
| DOXCUR-NP-3 | 300 | 5 ± 5 | 1.42 ± 0.03 | 1.61 ± 0.13 | 87.86 ± 2.76 | 96.85 ± 1.36 | 380.7 ± 0.3 | -16.2 ± 0.3 |
| DOXCUR-NP-4 | 200 | 2.5 ± 2.5 | 1.14 ± 0.05 | 1.18 ± 0.07 | 90.90 ± 4.21 | 96.76 ± 1.23 | 87.2 ± 0.1 | -20.8 ± 0.3 |
| DOXCUR-NP-5 | 200 | 5 ± 5 | 1.91 ± 0.13 | 2.29 ± 0.19 | 80.30 ± 1.82 | 96.21 ± 1.34 | 103.4 ± 0.3 | -11.7 ± 0.1 |
| DOXCUR-NP-6 | 200 | 7.5 ± 7.5 | 1.84 ± 0.21 | 6.61 ± 0.33 | 51.79 ± 2.68 | 94.51 ± 2.36 | 121.5 ± 0.2 | -8.2 ± 0.6 |

efficiency of DOX, more than 90%, was also obtained in all these formulations, and its loading content was easily adjusted, ranging from 1.18% to 6.61%. By contrast, it was more difficult for CUR to obtain the high the loading content and encapsulating efficiency because of a weak hydrophobic interaction between CUR and PLGA block. The drug-loading content and encapsulating efficiency of CUR was highly dependent on the ratio of CUR/copolymer in formulation. As the ratio of CUR/copolymer increased, the EE of CUR increased from 51.7% to 90.9%, while its loading content decreased accordingly from 2.61% to 1.14%. Because of high crystal properties for CUR, less than 5% of CUR loading in PLGA-based polymeric nanoparticles was also reported in these publications [21–23].

Particle size and zeta potentials of the blank nanoparticles (Blank NPs), single drug loaded nanoparticles (DOX-NPs; CUR-NPs) and series of dual-drugs loaded nanoparticles (CURDOX-NPs) were determined by DLS. The average size of the blank NPs was 211.2 ± 1.3 nm and the Zeta potential was -25.4 ± 0.2 mV. Compared with the blank NPs, the particle size of CUR-NPs increased slightly to 228.5 ± 1.5 nm, and its zeta potential (mV) was 23.8 ± 0.3 mV, which was not significantly different from that of blank NPs. By contrast, after loading DOX, D_h of DOX-NPs become smaller than the corresponding blank NPs, and its zeta potential increased inversely. D_h of DOX-NPs was reduced to 102.1 ± 0.4 nm and zeta potential increased to -21.2 ± 0.6 mV. Especially for series of CURDOX-NPs, with the increase in the ratio of DOX/copolymer, D_h of CURDOX-NPs decreased from 380.7 ± 0.3 nm to 56.2 ± 0.2 nm, while the zeta potential increased from -20.8 ± 0.3 mV to -5.2 ± 0.2 mV, as shown in Table 1. These results indicated denser solid nanoparticles were formed after drug loading due to the strong electrostatic interaction between DOX and the side carboxyl of PGLu. For the formulation (CURDOX-NPs-5), because of its advantageous characteristics such as a comparatively high DLC and EE for CUR and a suitable particle size and zeta potential, it was selected for the following studies.

The morphology of CURDOX-NPs

The morphology of the drug-loaded nanoparticles was determined by TEM. As indicated in Figure 1, sphere-shaped structures were observed for all the nanoparticles regardless of signal drug-loaded nanoparticles (CUR-NPs or DOX-NPs) or dual drugs loaded nanoparticles (CURDOX-NPs). For CUR-NPs,

TEM image clearly showed an evenly distributed spherical particles population and exhibited a smaller dried nanoparticle size (ca. 95 nm) than D_h determined by DLS (Figure 1(A)). This dried particle size was obviously smaller than that determined by DLS because of dehydration of the hybrid-core and shrinkage of the PEG shell induced by water evaporation under high vacuum before TEM measurement. However, for DOX-NPs or CURDOX-NPs, the dried particle size determined by TEM was slightly smaller with D_h determined by DLS. For example, a particle size just decreased from 103.4 nm of D_h to ca. 98 nm of dried nanoparticle size for CURDOX-NPs. Due to the dense solid core of these nanoparticles after DOX loading, it was only the dehydration of the PEG layer and not the hybrid core that was responsible for the reduced particle size in the dry state.

Drug crystal property inside CURDOX-NPs

The crystal status of the encapsulated DOX and CUR in polymeric nanoparticle was analysed by DSC and results were shown in Figure S1A. For pure drugs, the melting point (T_m) for DOX could be observed at 218°C , which was consistent with value reported in literature [24], whereas for CUR at 174.2°C as similar as results in the publication [17]. For mPEG-PLGA-PGLu copolymer, a wide endothermic peak at 58.6°C was attributed to the glass transition temperature (T_g) of PLGA block. Besides, there appeared a weak endothermic peak at 104°C , which corresponded to the temperature of the first-order transformation (TLC) between two stable helical conformations of PGLu block, from 7/2 to an 18/5 α -helical conformation [25]. The physical mixture of (CUR + DOX + Polymer) showed all the endothermic peaks that had been observed for the individual pure component. By contrast, for CURDOX-NPs, either T_m of DOX or CUR disappeared, indicating the molecular dispersion of the two crystal drugs (CUR and DOX) in nanoparticles. Meanwhile, T_{LC} of PGLu was also absent and only the peak ascribed to T_g of PLGA segment was observed, indicating co-encapsulation of PGLu together with DOX. The co-encapsulation of DOX together with PGLu was further confirmed by the fluorescence spectrum technique. The fluorescence intensity of the encapsulated DOX in CURDOX-NPs was significantly quenched, while it was instantly recovered when the nanoparticles were destroyed by DMF (Figure S1B), indicating localization of DOX inside the core of the nanoparticles. When DOX was encapsulated in nanocarriers, its self-fluorescence was quenched

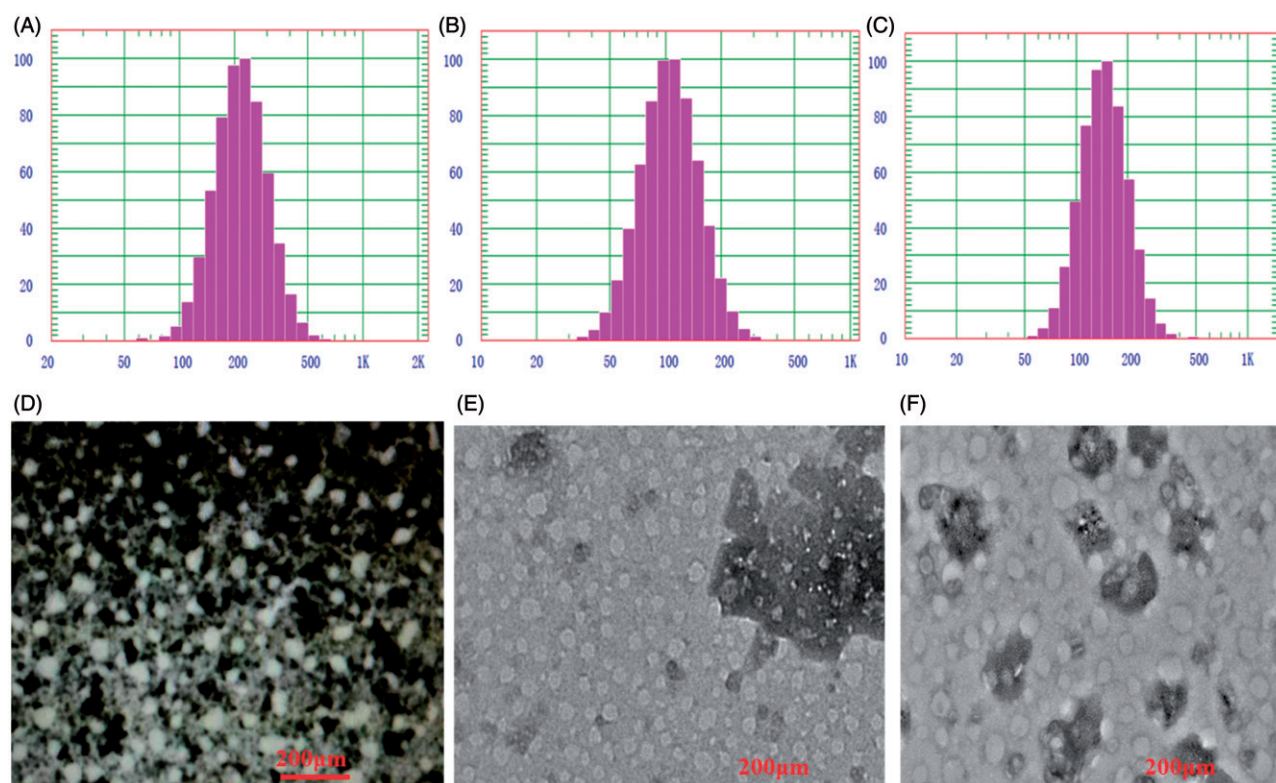


Figure 1. Particles size distribution and transmitted electronic microscopy (TEM) of CUR-NPs (A, D), DOX-NPs (B, E) and CURDOX-NPs (C, F).

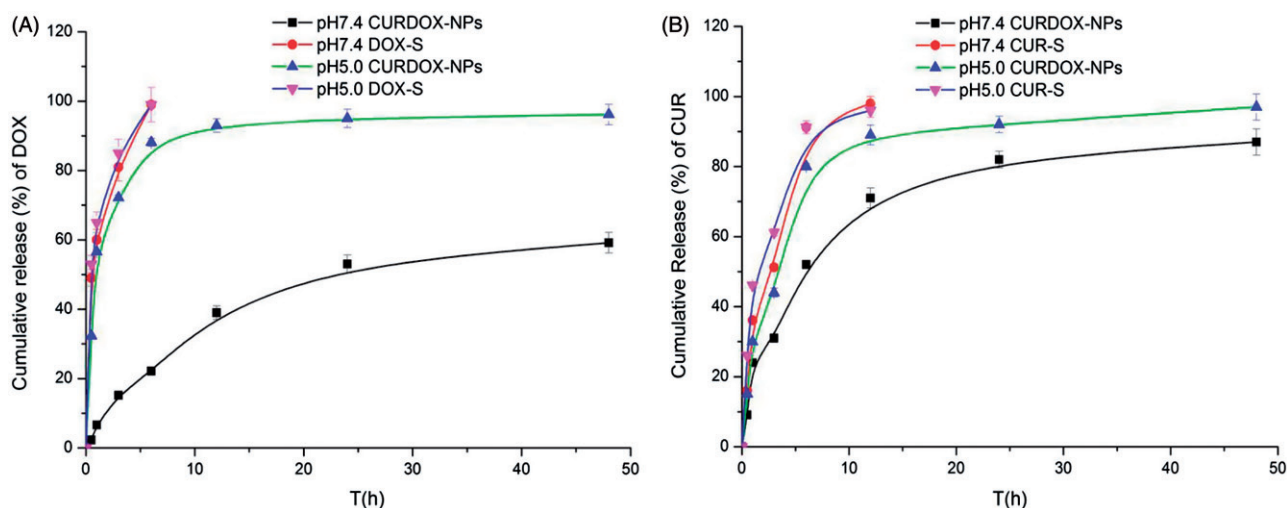


Figure 2. *In vitro* release profiles of DOX (A) and CUR (B) from nanoparticle formulation (CURDOX-NPs) or solution formulations (DOX-S or CUR-S) in pH7.4 PBS or pH5.0 acetate buffer.

because of a concentrated DOX aggregates in local micro-environment. The similar results were also obtained in these publications [26,27].

***In vitro* release profile of CUR and DOX from CURDOX-NPs**

The *in vitro* drug release profiles of CURDOX-NPs in pH7.4 PBS and pH5.0 acetate buffer were shown in Figure 2. A pH-sensitive release profile for each cargo from nanoparticles was seen regardless of CUR or DOX. In pH7.4 release medium, a slow release profile from CURDOX-NPs was observed for

both of CUR and DOX. Only 22% of the encapsulated DOX and 50% of the encapsulated CUR were released from CURDOX-NPs at 6 h, respectively, while more than 85% of CUR and DOX were released from their corresponding solution formulations (DOX-S or CUR-S) at 6 h. However, in pH5.0 acetate buffer, 85% of DOX and 80% of CUR was released from nanoparticles after 6 h, respectively. Meanwhile, a flocculate precipitate was formed in dialysis bag in the pH5.0 release medium. These suggested that the structure of CURDOX-NPs was destroyed in pH5.0 release medium due to protonation of the side carboxyl groups on the PGLu block. This hypothesis has been confirmed by TEM technique in our

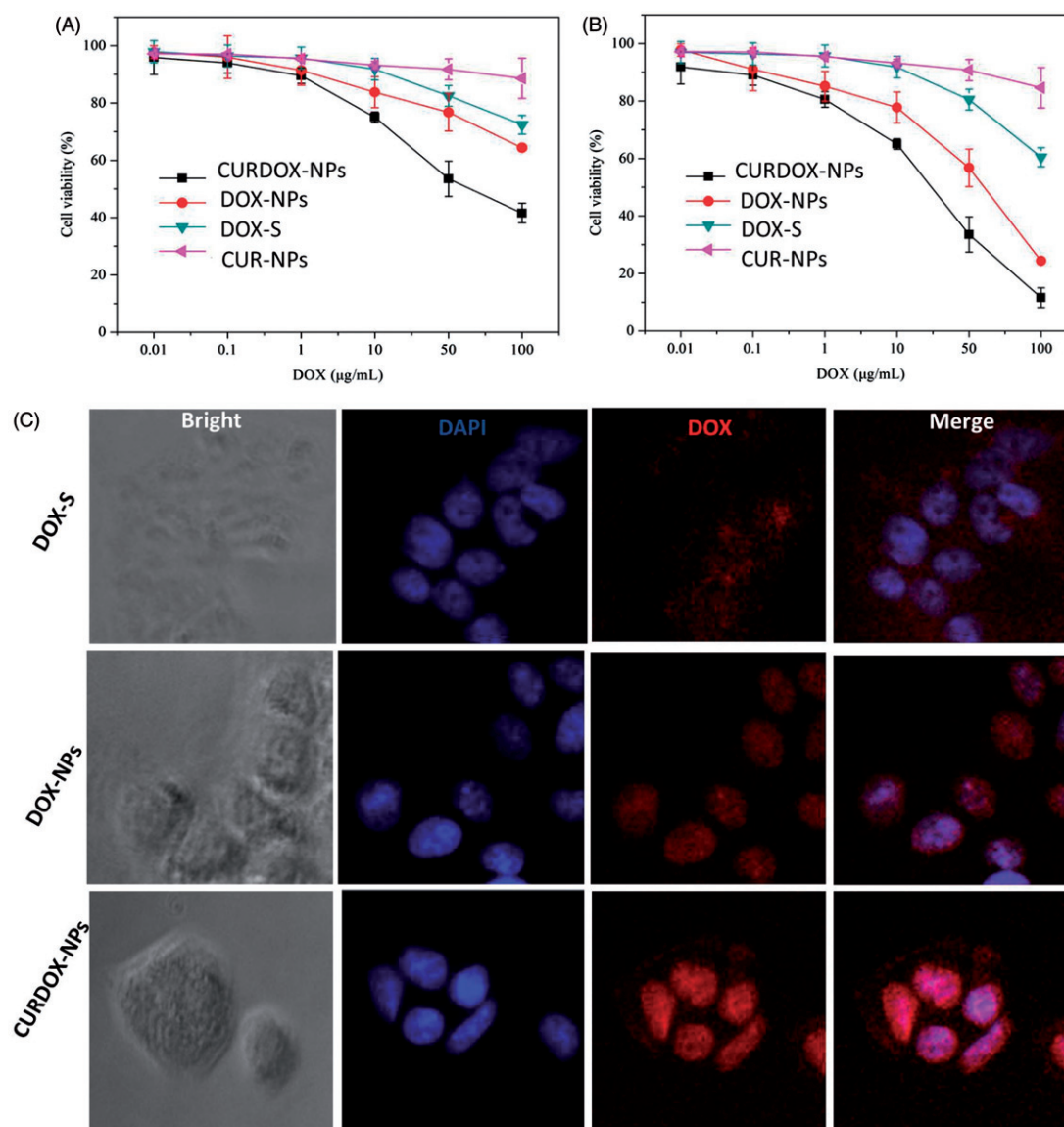


Figure 3. Cytotoxicity of the different formulation against MCF-7/ADR after incubation of 24 h (A) and 48 h (B), and (C) the fluorescent distribution of DOX in MCF-7/ADR cells after treatment with different formulations for 4 h at 37 °C.

previous study [18]. Interestingly, CUR release from nanoparticles was faster than DOX in pH7.4 release medium. This may due to the fact that the hydrophobic force between PLGA chain and CUR is weaker than the electrostatic interaction between PLGA segments with DOX, rendering ease of premature release of CUR. A faster release of CUR from PLGA-PEG nanoparticles was also observed in the similar study [28]. The cascading release profiles of two drugs with different therapeutic mechanism may be more in line with the needs of the practical treatment. For example, the treatment of drug-resistant tumours often require a faster release of P-gp inhibitor to increase the concentration of a slower release of chemotherapy drugs in these drug-resistant cells [29,30].

In vitro cytotoxicity and cellular uptake of CURDOX-NPs

MCF-7/ADR cell line has been demonstrated to be highly resistant against DOX in previous study [31]. To evaluate the therapeutic effect of the combination of CUR and DOX,

in vitro cytotoxicity of CURDOX-NPs against MCF-7/ADR after 24 h or 48 h of incubation was also evaluated in this study. The cytotoxicity of free DOX solution (DOX-S), single drug-loaded NPs including DOX-NPs or CUR-NPs against MCF-7/ADR were also tested for comparison. The results were shown in Figure 3(A,B). Except for CUR-NPs or DOX-S, a dose- and time-dependent cell proliferation inhibition against sensitive MCF-7/AR cells and DOX-NPs was more obviously exhibited for DOX-NPs or DSDDOX-NPs. After incubation of 24 h or 48 h, more than 80% of the cells were survival for CUR-NPs at the whole concentration range, indicating no obvious cytotoxicity against MCF-7/ADR. Despite a certain level of cell proliferation inhibition for DOX-S at high concentration, its IC_{50} values, a concentration at which 50% cells were killed, were highly reaching to 188.56 μg/mL at 24 h of incubation, indicating the strong resistance for MCF-7/ADR against DOX. By contrast, the sensitivity of MCF-7/ADR to DOX was enhanced when exposed to DOX-NPs. The IC_{50} value of DOX-NPs decreased to be 105 ± 1.2 μg/mL and 57.4 ± 1.0 μg/mL after

24 h and 48 h of incubation, respectively. Meanwhile, the dose-dependent cytotoxicity for CURDOX-NPs was displayed and its strongest cytotoxicity against MCF-7/ADR was observed among these formulations. The IC_{50} value of CURDOX-NPs was determined to be $52.4 \pm 2.7 \mu\text{g/mL}$ and $26.2 \pm 1.8 \mu\text{g/mL}$ after 24 h and 48 h of incubation, respectively, significantly lower than that of DOX-NPs. It could be noted that the IC_{50} value of CURDOX-NPs at 48 h was more than 2.2 times lower than that of DOX-NPs and 7.2 times lower than that of DOX-S.

Alternatively, in order to better demonstrate the reversal of multidrug resistance by curcumin, the cytotoxicity of these formulations against the sensitive MCF-7 cells were also studied and results were displayed in Figure S2. The MCF-7 cells were more sensitive to DOX-containing formulations in comparison with MCF-7/ADR cells line. All the DOX-containing formulations including DOX-S, DOX-NPs and CURDOX-NPs displayed dose- and time-dependent cell proliferation inhibition against sensitive MCF-7 cells and DOX-NPs exhibited the slightly enhanced cellular toxicity than that of free DOX-S. IC_{50} after treatment with all these formulation was comparable and estimated to be in range of $0.6 \mu\text{g/mL}$ to $1.1 \mu\text{g/mL}$, which was significantly lower than that observed in MCF-7/ADR cells line. As expectedly, the MCF-7 cells were less sensitive to curcumin-containing formulation (CUR-NPs) than DOX-containing formulations. The calculated IC_{50} values were $31.60 \pm 1.21 \mu\text{g/mL}$ and $13.41 \pm 1.21 \mu\text{g/mL}$ after 24 h and 48 h treatment with CUR-NPs, respectively. The resulting IC_{50} of CUR-NPs was comparable to that of curcumin encapsulated in pH-responsive chitosan mesoporous silica nanoparticles in publication [32]. But cytotoxicity of CUR-NPs against MCF-7 cells was higher than that against MCF-7/ADR.

Cellular uptake of CURDOX-NPs

Furthermore, the cellular uptake of CURDOX-NPs by MCF-7/ADR cells was also examined by laser confocal microscopy after 4 h of incubation at 37°C . Results were displayed in Figure 3(C). A faint DOX fluorescence was distributed inside cytoplasm of MCF-7/ADR and the DOX was seldom transported to cellular nuclei, where its active target resided. The localized drug efflux pumps such as P-gp, were over-expressed on cellular membrane of MCF-7/ADR cells, which were responsible for recognizing the chemotherapeutic agents and pumping them out of cells, leading to the very low drug concentration in target sites. On the contrary, DOX encapsulated in polymeric nanoparticles could enter the cell via endocytosis, bypassing the direct recognition of P-gp. Thus, it was seen that more DOX was distributed to cellular nuclei for DOX-NPs (Figure 3(C)). But it was reported that a part of endocytosed drug near cytoplasm membrane was still recognized and pumped out. CURDOX-NPs can first release CUR to suppress P-gp pumps and prevent exclusion of DOX out of cells. Therefore, a significant DOX fluorescence was observed inside nuclei of MCF-7/ADR after treated with CURDOX-NPs, even though the concentration of DOX in CURDOX-NPs was equivalent with DOX-NPs ($10 \mu\text{g/mL}$). Massive DOX distribution for CURDOX-NPs in nuclear

compartments resulted in its strong cytotoxicity against MCF-7/ADR DOXCUR-NPs.

As control, the cellular uptake of these formulations by sensitive MCF-7 cells was also examined by laser confocal microscopy after 4 h of incubation at 37°C . Results were shown in Figure S3. There was excessive red fluorescence of DOX distributed inside the cellular nuclei of MCF-7 cells treated with these formulations. Moreover, no significant difference in cellular fluorescent intensity was observed between these cells treated with various formulations. These results suggested DOX regardless of free form or the encapsulated form was easily uptaken by sensitive MCF-7 cells.

Enrichment and identification of breast cancer stem cells

The spheroid-forming culture (mammosphere for breast cancer) has also been used to isolate or enrich breast CSCs [33]. This is a useful method for studying the properties of breast CSCs and therapeutic strategies that target them [34,35]. In this study, mammosphere of MCF-7/ADR was successfully cultured on 2% agarose hydrogel, as shown in Figure S4A. After 7 days of culture, mammosphere gradually grow to be approximately $800 \mu\text{m}$ of diameter and were digested using trypsin for identification of breast cancer stem cell line. Figure S4B displays the phenotype of the mammosphere-derived MCF-7/ADR cancer stem cells identified with high expression of CD44 (marked as $CD44^+$) but low expression of CD24[−] (marked as $CD24^-$). The $CD44^+/CD24^-$ cells were the tumorigenic stem cells and identified as the breast cancer stem cells by flow cytometry. The purity of MCF-7/ADR cancer stem cells dissociated from the mammospheres in serum-free culture medium was 45.1%, while it was only 4.36% for the typical adherent MCF-7/ADR cells (Figure S4C).

Growth inhibition of mammosphere and killing heterogeneous tumour cells by CURDOX-NPs

In vitro growth inhibition of MCF-7/ADR mammosphere was investigated after treatment with different formulations. Results were exhibited in Figure 4(A,B). the size and volume of mammospheres of MCF-7/ADR were reduced as compared with those applying PBS (pH7.4, blank control). CURDOX-NPs exhibited the most powerful inhibition of tumour spheroid growth. Just at the third day after treatments, it was observed that the tumour spheroids with PBS grew rapidly, with volumes as high as 1.6 times its primary volume. In contrast, an obvious growth inhibition of mammosphere was observed in a group treated with various drug-loaded NPs formulations. The volumes of mammosphere on day 3 were only 1.2, 0.9 and 0.5 times that of the primary volume after treatment with CUR-NPs, DOX-NPs and the CURDOX-NPs, respectively. The representative images observed under an inverted microscope were in agreement with the quantitative data. This enhanced effect of CURDOX-NPs might be caused by the enhanced DOX concentration in drug-resistant MCF-7/ADR cells because of the targeting ability of CUR against efflux pump, P-gp.

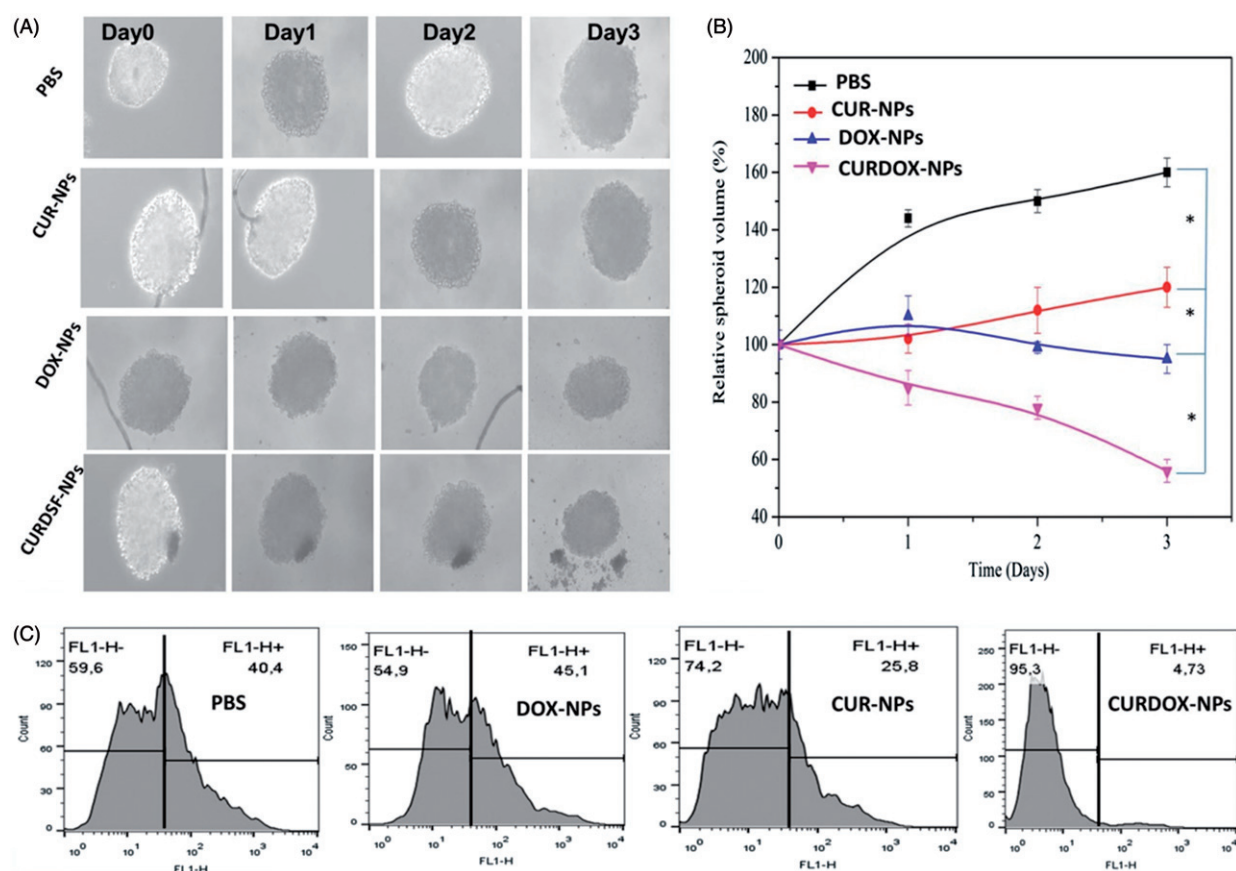


Figure 4. (A) microscopic images and (B) the relative spheroid volume of MCF-7/ADR spheroid after treatment with different formulations, and (C) the percentage of CD44⁺/CD24⁻ cells in MCF-7/ADR mammospheres after 3 days of treatment with various formulations. The dissociated MCF-7/ADR mammosphere cells were stained with anti-CD44-FITC and anti-CD24-PE antibodies.

Accordingly, to confirm whether the heterogeneous tumour cells were killed in breast cancer, after 3 days of treatment, the surface markers expression of the dissociated MCF-7/ADR mammosphere cells were further analysed by flow cytometry. Results were shown in Figure 4(C). The percentage of CD44⁺/CD24⁻ cells was increased by the DOX-NPs treatment compared to the control group; conversely, the CD44⁺/CD24⁻ cells percentage was decreased to a great extent by the CUR-NPs or CURDOX-NPs treatments (Figure 4(C)). Furthermore, the CURDOX-NPs treatment was significantly more effective at reducing the CD44⁺/CD24⁻ cells population than the CUR-NPs treatment. This was due to the fact that massive killing of the common breast cancer cells made more CUR be available by the concealed breast cancer stem cells in mammospheres.

In vivo antitumour effect

The *in vivo* anti-tumour efficacy of normal saline (Control), CUR-NPs, DOX-NPs and CURDOX-NPs was evaluated in MCF-7/ADR tumour-bearing mice. As shown in Figure 5, tumours treated with saline grow faster than that in other groups. Both single drug-loaded nanoparticle of CUR-NPs and DOX-NPs showed significant inhibition of tumor growth compared with the saline group ($p < .05$). Moreover, DOX-NPs exhibited a better inhibition of tumour growth than CUR-NPs. By contrast, CURDOX-NPs treatment produced the slowest tumour

growth in MCF-7/ADR tumour-bearing mice. Meanwhile, the tumour weight for the CURDOX-NPs group was significantly lower than that of other groups, which was in agreement with the tumour growth inhibition results, indicating its best anti-tumour effect. Despite not the first-line chemotherapeutic agent, the anticancer efficacy of CUR was proved through inhibiting NF- κ B pathway and targeting breast cancer stem cells *in vitro* and *in vivo* [11]. Especially, when CUR combined with the first-line chemotherapeutic drug (DOX), the most effective inhibitory effect on the growth of drug-resistant breast cancer xenografts was reported due to the enhanced distribution of DOX through inhibition of P-gp [36].

Animal body weight changes were used as a marker of the toxicity of anti-tumor therapeutic agents in tumour-bearing animals. The body weight loss, less than 10%, was low for mice treated with all these formulations at total drug dose of 2.5 mg/kg/each time, confirming the low systemic toxicity of all these formulations. The low toxicity against normal tissues, especially heart, may be associated with the low administered dose of DOX.

Anti-proliferative effect of CURDOX-NPs on cancer stem cells in vivo

The cells population recovered from the tumours at the end of the treatments was analysed. As shown in Figure S5, the percentage of cancer stem cells from mice treated with

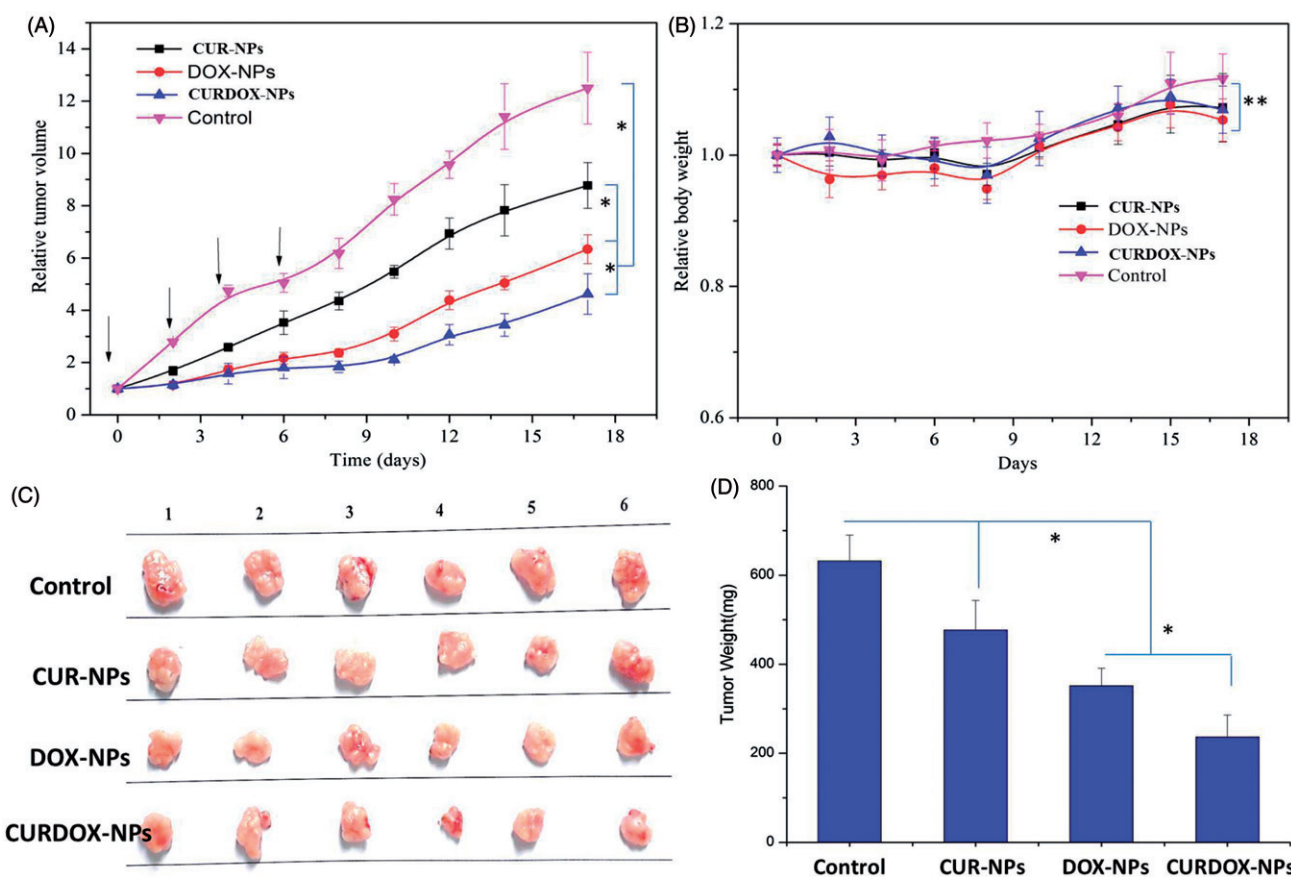


Figure 5. *In vivo* anti-tumour efficacy of various formulations, (A) tumour growth of MCF-7/ADR cancer xenografts treated with saline (control), CUR-NPs, DOX-NPs and CURDOX-NPs at a total drug dose of 2.5 mg/kg; (B) the loss of body weight of tumour-bearing mice after treatment; (C) tumour image and (D) tumour weight excised at 17 days post-treatment ($n = 6$, $p < .05$).

CUR-NPs or CURDOX-NPs was significantly lower than that of the control group. The percentage of cancer stem cells in the tumours treated with CURDOX-NPs was lower than that in the tumours treated with CUR-NPs (15.0% vs. 6.82%), attributing to more availability of CUR by the concealed breast cancer stem cells after DOX-induced destruction of the common breast cancer cells *in vivo*. In contrast, after the treatment with DOX-NPs, the percentage of cancer stem cells was much higher than that of the control group, which was consistent with findings reported by others [37,38].

Toxicity of CURDOX-NPs against normal tissues

To evaluate the toxicity of CURDOX-NPs, pathological HE-stained sections from the heart, liver, spleen, lung and kidney were assayed (Figure S6). Regardless of treatment with single drug-loaded nanoparticles (CUR-NPs/DOX-NPs) or dual drugs-loaded nanoparticles (CURDOX-NPs), there was not any noticeable organ damage or inflammatory lesions in the heart, liver, spleen, lung or kidney of rats, indicating that CURDOX-NPs did not cause significant toxicity in the treated rats.

Conclusions

Recently, cancer stem cells (CSCs) have been considered to be a source for initiation, invasion, metastasis and recurrence

of breast tumour [39,40]. It has become a new strategy to simultaneously target the CSCs and the differentiated tumour cells by concomitant delivery of CSCs-targeting agents and traditional chemotherapeutics. Doxorubicin hydrochloride has been used as first-line drug against breast cancer. Curcumin was reported to specifically target CSC-like cell populations in tumor. The use of CUR as a chemical sensitizer in combination with doxorubicin can improve antitumor efficacy against refractory breast cancer and reduce DOX-induced cardiac toxicity. But whether the therapeutic mechanism of combinational treatment was associated with cancer stem cells has not been clarified. Moreover, in view of existence of inconsistent pharmacokinetics profiles between CUR and DOX, there are few strategies with high efficiency and ability to simultaneously deliver them into breast tumor tissue in clinical treatment, which may compromise their anti-tumour effect.

In this study, a pH-sensitive dual drug-loaded nanoparticle with simultaneous encapsulation of curcumin and doxorubicin (CURDOX-NPs) was prepared by using monomethoxy (polyethylene glycol)-b-P (D,L-lactic-co-glycolic acid)-b-P (L-glutamic acid) polymer (mPEG-PLGA-PGLu) to simultaneously target the breast cancer stem cells and the differentiated tumour cells. Despite of the tremendous difference in physicochemical properties between CUR and DOX, the definite drug loading sites for mPEG-PLGA-PGLu copolymer, for example, PLGA segment for CUR loading and PGLu block for DOX loading, render the nanoparticles reaching high drug-loading

efficiency for each cargo. Moreover, CURDOX-NPs exhibited a cascade sustained-release profiles with the faster release of CUR followed by a slower release of DOX was observed in normal pH7.4 condition. Meanwhile, a pH-sensitive release profile of each cargo from nanoparticles was seen in tumour-associated pH5.0 condition. These release behaviour was beneficial to enhance DOX distribution in tumour, thus resulting in massive killing of the differentiated tumour cells. The effective anti-tumour effect of CURDOX-NPs on refractory MCF-7/ADR-bearing Xenograft mice model was confirmed by *in vitro*. The percentage of cancer stem cells in the tumours significantly decreased from 39.9% in control group to 6.82% after treatment with CURDOX-NPs, indicating the simultaneous killing of heterogeneous tumour cells in breast cancer. The combinational delivery of CUR and DOX may a potentially useful therapeutic strategy for refractory breast cancer.

Disclosure statement

There are no conflicts of interest to declare.

Funding

This research was supported by National Natural Science Foundation of China (Grant No. 81603036 and 81571392), Natural Science Foundation of Zhejiang Province (Grant No. LY17H180008), key research and development program of Zhejiang province (Grant No. 2018C03013), Medicine Grant from Wenzhou Municipal Science and Technology Bureau (Grant No. Y20160086), School Talent Start Fund of Wenzhou Medical University (Grant No. QTJ15020).

References

- Izrailit J, Reedijk M. Developmental pathways in breast cancer and breast tumor-initiating cells: therapeutic implications. *Cancer Lett*. 2012;317:115–126.
- Zhao Y, Alakhova DY, Kabanov AV. Can nanomedicines kill cancer stem cells? *Adv Drug Deliv Rev*. 2013a;65:1763–1783.
- Meng F, Zhong Y, Cheng R, et al. pH-sensitive polymeric nanoparticles for tumor-targeting doxorubicin delivery: concept and recent advances. *Nanomedicine (Lond)*. 2014;9:487–499.
- Wang Y, Wei X, Zhang C, et al. Nanoparticle delivery strategies to target doxorubicin to tumor cells and reduce side effects. *Ther Deliv*. 2010;1:273–287.
- Xu H, Yao Q, Cai C, et al. Amphiphilic poly(amino acid) based micelles applied to drug delivery: the *in vitro* and *in vivo* challenges and the corresponding potential strategies. *J Control Release*. 2015c;199:84–97.
- El-Rayes BF, Ibrahim D, Shields AF, et al. Phase I study of liposomal doxorubicin (Doxil) and cyclophosphamide in solid tumors. *Invest New Drugs*. 2005;23:57–62.
- Alakhova DY, Zhao Y, Li S, et al. Effect of doxorubicin/pluronic SP1049C on tumorigenicity, aggressiveness, DNA methylation and stem cell markers in murine leukemia. *PLoS One*. 2013;8:e72238.
- Matsumura Y. [Micelle carrier system in clinical trial]. *Nihon Rinsho*. 2006;64:316–321.
- Xu HL, Fan ZL, ZhuGe DL, et al. Therapeutic supermolecular micelles of vitamin E succinate-grafted epsilon-polylysine as potential carriers for curcumin: Enhancing tumour penetration and improving therapeutic effect on glioma. *Colloids Surf B Biointerfaces*. 2017;158:295–307.
- Jiao Y, Hannafon BN, Ding WQ. Disulfiram's Anticancer Activity: Evidence and Mechanisms. *Anticancer Agents Med Chem*. 2016;16:1378–1384.
- Liu P, Wang Z, Brown S, et al. Liposome encapsulated Disulfiram inhibits NFkappaB pathway and targets breast cancer stem cells *in vitro* and *in vivo*. *Oncotarget*. 2014;5:7471–7485.
- Yang Z, Sun N, Cheng R, et al. pH multistage responsive micellar system with charge-switch and PEG layer detachment for co-delivery of paclitaxel and curcumin to synergistically eliminate breast cancer stem cells. *Biomaterials*. 2017;147:53–67.
- Han D, Wu G, Chang C, et al. Disulfiram inhibits TGF-beta-induced epithelial-mesenchymal transition and stem-like features in breast cancer via ERK/NF-kappaB/Snail pathway. *Oncotarget*. 2015; 6:40907–40919.
- Wang Z, Tan J, McConville C, et al. Poly lactic-co-glycolic acid controlled delivery of disulfiram to target liver cancer stem-like cells. *Nanomedicine*. 2017;13:641–657.
- Zhu JY, Yang X, Chen Y, et al. Curcumin suppresses lung cancer stem cells via inhibiting Wnt/beta-catenin and sonic Hedgehog pathways. *Phytother Res*. 2017;31:680–688.
- Zhang L, Tian B, Li Y, et al. A copper-mediated disulfiram-loaded pH-triggered PEG-shedding TAT peptide-modified lipid nanocapsules for use in tumor therapy. *ACS Appl Mater Inter*. 2015;7:25147–25161.
- Jing G, Zhong Y, Zhang L, et al. Increased dissolution of disulfiram by dry milling with silica nanoparticles. *Drug Dev Ind Pharm*. 2015;41:1328–1337.
- Xu H, Cai C, Gou J, et al. Self-assembled monomethoxy (polyethylene glycol)-b-P(D,L-lactic-co-glycolic acid)-b-P(L-glutamic acid) hybrid-core nanoparticles for intracellular pH-triggered release of doxorubicin. *J Biomed Nanotechnol*. 2015a;11:1354–1369.
- Xu H, Yang D, Cai C, et al. Dual-responsive mPEG-PLGA-PGLu hybrid-core nanoparticles with a high drug loading to reverse the multidrug resistance of breast cancer: an *in vitro* and *in vivo* evaluation. *Acta Biomater*. 2015b;16:156–168.
- Xu HL, Mao KL, Lu CT, et al. An injectable acellular matrix scaffold with absorbable permeable nanoparticles improves the therapeutic effects of docetaxel on glioblastoma. *Biomaterials*. 2016;107:44–60.
- Adahoun MA, Al-Akhras MH, Jaafar MS, et al. Enhanced anti-cancer and antimicrobial activities of curcumin nanoparticles. *Artif Cells Nanomed Biotechnol*. 2017;45:98–107.
- Farajzadeh R, Pilehvar-Soltanahmadi Y, Dadashpour M, et al. Nano-encapsulated metformin-curcumin in PLGA/PEG inhibits synergistically growth and hTERT gene expression in human breast cancer cells. *Artif Cells Nanomed Biotechnol*. 2017. [Epub ahead of print]. DOI: [10.1080/21691401.2017.1347879](https://doi.org/10.1080/21691401.2017.1347879)
- Liang H, Friedman JM, Nacharaju P. Fabrication of biodegradable PEG-PLA nanospheres for solubility, stabilization, and delivery of curcumin. *Artif Cells Nanomed Biotechnol*. 2017;45:297–304.
- Wang JL, Sun J, Chen Q, et al. Star-shape copolymer of lysine-linked di-tocopherol polyethylene glycol 2000 succinate for doxorubicin delivery with reversal of multidrug resistance. *Biomaterials*. 2012;33:6877–6888.
- Xu HL, Fang GH, Gou JX, et al. Lyophilization of self-assembled polymeric nanoparticles without compromising their microstructure and their *in vivo* evaluation: pharmacokinetics, tissue distribution and toxicity. *J Biomater Tissue Eng*. 2015d;5:919–929.
- Han K, Zhang WY, Zhang J, et al. pH-responsive nanoscale coordination polymer for efficient drug delivery and real-time release monitoring. *Adv Healthc Mater*. 2017;6:1700471–1700479.
- Zhao Y, Alakhova DY, Kim JO, et al. A simple way to enhance Doxil (R) therapy: Drug release from liposomes at the tumor site by amphiphilic block copolymer. *J Controlled Release*. 2013b;168:61–69.
- Mirakabad FST, Akbarzadeh A, Milani M, et al. A Comparison between the cytotoxic effects of pure curcumin and curcumin-loaded PLGA-PEG nanoparticles on the MCF-7 human breast cancer cell line. *Artif Cells Nanomed Biotechnol*. 2016;44:423–430.
- Kang XJ, Wang HY, Peng HG, et al. Codelivery of dihydroartemisinin and doxorubicin in mannosylated liposomes for drug-resistant colon cancer therapy. *Acta Pharmacol Sin*. 2017;38:885–896.

- [30] Wang N, He T, Shen YM, et al. Paclitaxel and tacrolimus coencapsulated polymeric micelles that enhance the therapeutic effect of drug-resistant ovarian cancer. *Acs Appl Mater Inter*. 2016; 8:4368–4377.
- [31] Hong W, Chen D, Zhang X, et al. Reversing multidrug resistance by intracellular delivery of Pluronic(R) P85 unimers. *Biomaterials*. 2013;34:9602–9614.
- [32] Nasab NA, Kumleh HH, Beygzadeh M, et al. Delivery of curcumin by a pH-responsive chitosan mesoporous silica nanoparticles for cancer treatment. *Artif Cells Nanomed Biotechnol*. 2017. [Epub ahead of print]. DOI: [10.1080/21691401.2017.1290648](https://doi.org/10.1080/21691401.2017.1290648)
- [33] Burke AR, Singh RN, Carroll DL, et al. The resistance of breast cancer stem cells to conventional hyperthermia and their sensitivity to nanoparticle-mediated photothermal therapy. *Biomaterials*. 2012;33:2961–2970.
- [34] Wang D, Huang JB, Wang XX, et al. The eradication of breast cancer cells and stem cells by 8-hydroxyquinoline-loaded hyaluronan modified mesoporous silica nanoparticle-supported lipid bilayers containing docetaxel. *Biomaterials*. 2013;34:7662–7673.
- [35] Zhang Y, Zhang H, Wang XQ, et al. The eradication of breast cancer and cancer stem cells using octreotide modified paclitaxel active targeting micelles and salinomycin passive targeting micelles. *Biomaterials*. 2012;33:679–691.
- [36] Duan X, Xiao J, Yin Q, et al. Smart pH-sensitive and temporal-controlled polymeric micelles for effective combination therapy of doxorubicin and disulfiram. *ACS Nano*. 2013;7:5858–5869.
- [37] Hirsch HA, Iliopoulos D, Struhl K. Metformin inhibits the inflammatory response associated with cellular transformation and cancer stem cell growth. *Proc Natl Acad Sci USA*. 2013; 110:972–977.
- [38] Ke XY, Lin Ng VW, Gao SJ, et al. Co-delivery of thioridazine and doxorubicin using polymeric micelles for targeting both cancer cells and cancer stem cells. *Biomaterials*. 2014;35:1096–1108.
- [39] Haynes B, Sarma A, Nangia-Makker P, et al. Breast cancer complexity: implications of intratumoral heterogeneity in clinical management. *Cancer Metastasis Rev*. 2017;36:547–555.
- [40] Toss M, Miligy I, Thompson AM, et al. Current trials to reduce surgical intervention in ductal carcinoma in situ of the breast: critical review. *Breast*. 2017;35:151–156.